The Voronoi tessellation generated from eigenvalues of complex random matrices

1990 J. Phys. A: Math. Gen. 23 3279

(http://iopscience.iop.org/0305-4470/23/14/025)

J. Phys. A: Math. Gen. **23** (1990) 3279-3295. Printed in the UK

The Voronoi tessellation generated from eigenvalues of complex random matrices

G Le Caër† and J S Ho‡

HLRZ, Forschungszentrum Jülich, Postfach 1913, D-5170 Jülich 1, Federal Republic of Germany

Received 27 December 1989

Abstract. The Voronoi froth generated from eigenvalues of asymmetric complex random matrices is studied by numerical simulation. It is more regular than the random Voronoi froth (RVF) generated from a Poisson process. The existence of a unique tessellation, called here random matrix Voronoi froth (RMVF), follows from the universality of the distribution of eigenvalues, which is also briefly commented on. The geometrical and topological properties of the RMVF have been characterised. An empirical and accurate distribution function is also proposed for the cell side length of a RVF. Deviations from the Aboav-Weaire law are discussed. Their magnitude may be interpreted as a measure of the departure from an equilibrium structure in the frame of the statistical crystallography theory of Rivier.

1. Introduction

The Voronoi tessellations with respect to a Poisson process in D-dimensional spaces (D from 2 to 4) are of interest in many fields including, for example, materials science (Meijering 1953, Wray *et al* 1983, DiCenzo and Wertheim 1989), geography (Getis and Boots 1979), quantum field theory (Christ *et al* 1982, Drouffe and Itzykson 1984), biology (Honda 1978), statistics (Ripley 1981, Stoyan *et al* 1987), etc. Such tessellations, called here random Voronoi froths (RVF, Rivier 1985), are determined by Poisson distributed points such that each point has associated with it the region of space nearer to that point than to any other point. The Poisson point process is characterised by (Stoyan *et al* 1987):

(a) the number of points in any finite region of 'volume' V has a Poisson distribution of mean ρV, where ρ is the density;

(b) the numbers of points of the process in k disjoint regions are k independent random variables.

The present paper will focus on two-dimensional space-filling random cellular structures. The 2D random Voronoi froth belongs to such structures. It is unique, in the statistical sense and easy to construct. However, it has a very different appearance from all spacefilling natural structures (Weaire and Rivier 1984). In order to describe such natural structures, Rivier (1985) has applied the methods of statistical mechanics. He has tried to determine the equilibrium structures using maximum entropy inference

† Permanent address and address for correspondence: LSG2M, associé au CNRS UA 159, Ecole des Mines, F-54042 Nancy Cedex, France.

‡ Address after 1 January 1990: Department 48B/428, IBM, Kingston, New York 2401, USA.

0305-4470/90/143279+17$03.50

under few constraints such as space-filling, Euler's relation (mean number of cell sides $\langle n \rangle = 6$), correlations between cell sizes and shapes etc (see also De Almeida and Iglesias 1988, 1989). Statistical crystallography, as named by Rivier, has, however, not yet completely solved the difficult problems related to subtle correlations in the organisation of the cells. As emphasised by Rivier (1985), the RVF structure is spacefilling by construction rather than through a constraint. As the random Voronoi froth is rapidly relaxed to equilibrated structures, Rivier has suggested that the RVF is a young structure which has not fully equilibrated itself under the influence of constraints.

In order to know if all Voronoi tessellations show the same features, it is interesting to construct a Voronoi tessellation which looks more closely like natural structures. Such a tessellation must also be isotropic, homogeneous and easy to construct by computer simulation. We argue, in the present work, that the Voronoi tessellation associated with the eigenvalues of complex random matrices, called here random matrix Voronoi froth (RMVF) allows the defining of such a structure. The RMVF is also unique in the statistical sense (section 2). It is intermediate between complete disorder and complete order. In a related paper (Le Caër 1990), we will show that the point process associated with the eigenvalues of complex random matrices may be applied to the statistical study of natural point processes such as positions of trees in forests, sea-bird nests, graphite nodules in cast iron, etc. This is a further argument which makes the RMVF noteworthy.

We will first describe some properties of the distribution of eigenvalues of complex random matrices. As for every random cellular structure, we will characterise various geometrical (area, perimeter, side length) and topological (side number, correlations among cells) distributions. We will also discuss two important semi-empirical laws, the Aboav–Weaire law (Aboav 1970, Weaire 1974) and the Lewis–Rivier law (Lewis 1928, Rivier and Lissowski 1982, Rivier 1983, 1985). Extended numerical results are given. They may be helpful to test future theoretical models.

2. Distribution of eigenvalues of complex random matrices

Random matrices (Mehta 1967) were widely studied in the 1960s in order to model the fluctuations of highly excited nuclear energy levels and have since been applied to fluctuations of energy levels in various situations and to the study of chaos (Seligman and Nishioka 1986). The distribution of eigenvalues of complex Gaussian random matrices has been calculated mathematically by Ginibre (1965) and Mehta (1967). It has also been discussed recently in the context of quantum chaos (Sommers *et al* 1988, Grobe *et al* 1988, Grobe and Haake 1989). In all cases, the eigenvalues show a repulsion effect, characterised by a zero probability of finding two identical eigenvalues. In the case of real eigenvalues, this repulsion may be tuned by changing the symmetry properties of the matrix ensemble. Due to the repulsion effect, eigenvalue patterns are more regular than the Poisson point pattern. The Voronoi tessellation generated from complex eigenvalues cannot in fact be discriminated from biological tissues by a simple visual inspection (figure 1) although differences are clearly seen in table 1.

We first consider an ensemble of $N \times N$ fully asymmetric complex matrices M_N with elements $m_{ij}(N)$ whose real and imaginary parts are independently distributed according to a Gaussian distribution with mean $m = 0$ and standard deviation $\sigma/\sqrt{2}$. The joint probability density for the eigenvalues $z_1, \ldots, z_N$ as well as the n-point

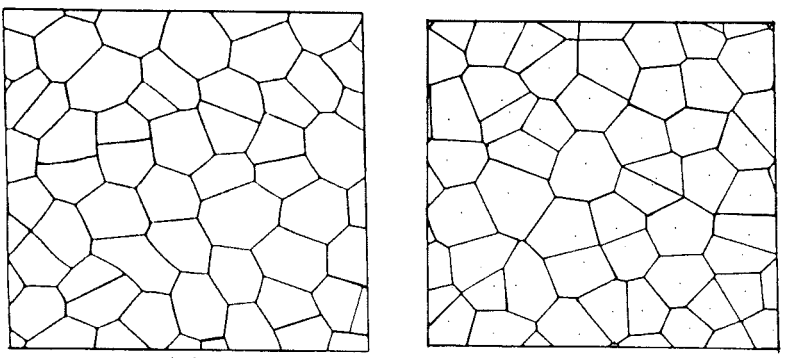

Figure 1. (*a*) Cells from the epidermal epithelium of the cucumber (after Lewis 1928). (*b*) Voronoi tessellation generated from a complex Gaussian random matrix.

Table 1. Proportions p_n of the number of sides n for various froths.

	$n=3$	$n=4$	$n=5$	$n=6$	$n=7$	$n=8$	$n=9$	$n=10$	$n=11$
EC†	—	0.020	0.251	0.474	0.224	0.030	0.001	—	—
RMVF	0.0022 (2)	0.069 (1)	0.2676 (16)	0.356 (3)	0.217 (1)	0.0715 (9)	0.0147 (7)	0.0019 (3)	15×10^{-5} (7)
RVF	0.0113 (2)	0.1068 (2)	0.2595 (5)	0.2946 (3)	0.1986 (1)	0.0905 (3)	0.0295 (3)	0.0074 (1)	144×10^{-5} (3)

† Epithelium cucumis 1000 cells (Lewis 1928).

correlation function R_n have been calculated by Ginibre (1965) (see also Mehta 1967, chapter 12). When $N\to\infty$, the correlation function R_n approaches well defined limits:

$$R_n(z_1,\ldots,z_n)=(\pi\sigma^2)^{-n}\exp\left(-\sum_{i=1}^{n}\frac{|z_i|^2}{\sigma^2}\right)\det[\exp(z_i z_j^*/\sigma^2)]_{i,j=1,\ldots,n}. \quad (1)$$

The density $R_1(z)$ is isotropic, nearly constant and equal to the asymptotic value $1/\pi\sigma^2$ ($N\to\infty$) for $r(=|z|)\leqslant\sigma N^{1/2}$ and goes to zero in an interval of order σ around $\sigma N^{1/2}$ (figure 2) (Ginibre 1965). This is particularly important for numerical simulations whose aim is to produce the best approximation of the properties expected for infinite N with a finite N value. It is readily verified that

$$R_n(z_1,\ldots,z_n)=R_n(z_1+a,\ldots,z_n+a) \quad (2)$$

when $N\to\infty$, whatever n and the complex number a. When $N\to\infty$, $R_n\to(\pi\sigma^2)^{-n}$ for large distances, approaching therefore to the value of the n-point correlation function of a Poisson process with a density $\rho=(\pi\sigma^2)^{-1}$. The eigenvalues are thus uncorrelated for large distances. The point process associated with the eigenvalues is isotropic whatever N and also homogeneous in the limit $N\to\infty$ (relations (1) and (2), Ginibre 1965, Mehta 1967).

As shown by Ginibre (1965), the previous distribution of eigenvalues is identical with the distribution of the positions of charges of a two-dimensional Coulomb gas in a harmonic oscillator potential, at a temperature $kT=0.5$. It is therefore a Gibbs point process in the plane (Stoyan *et al* 1987) for which the interaction potential does not reduce to a pair potential.

Some conditions, under which an universal distribution of complex eigenvalues of this type is obtained, have been discussed recently. As our numerical simulations give

some new information about this problem, we will discuss it briefly. For finite N, the eigenvalues are approximately located in a disc (figure 3(a)).

If S_N is the spectral radius of the matrix $M_N/\sqrt{N}$, then

$$\lim_{N\to\infty} S_N = \sigma \tag{3}$$

almost surely (Hwang 1986), i.e. S_N converges to σ with probability 1. Hwang has conjectured that (3) remains valid under suitable moment conditions for independently and identically distributed (IID) matrix elements, such that:

$$\begin{aligned} &\langle m_{ij}(N)\rangle = 0 \qquad \langle |m_{ij}(N)|^2\rangle = \sigma^2 \\ &\langle |m_{ij}(N)|^p\rangle \leqslant p^{\alpha p} \qquad \text{for all } p \geqslant 2 \text{ and some } \alpha. \end{aligned} \tag{4}$$

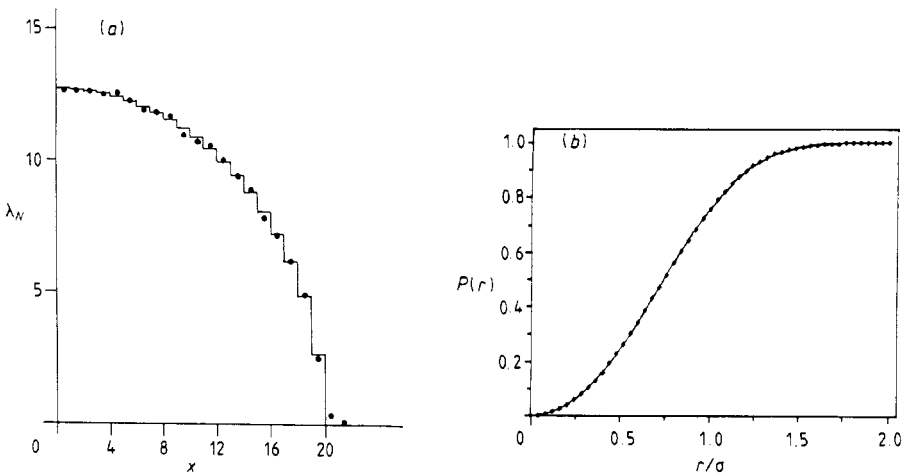

Figure 2. (a) Generalised semicircle law: histograms calculated from equation (5) with $N = 400$. Points: average values from numerical simulations (50 matrices, $N = 400$). (b) Cumulative distribution of the distance from a point taken at random to the nearest eigenvalue. Points: simulation, full curve: calculated from equation (9) ($\sigma = 1$).

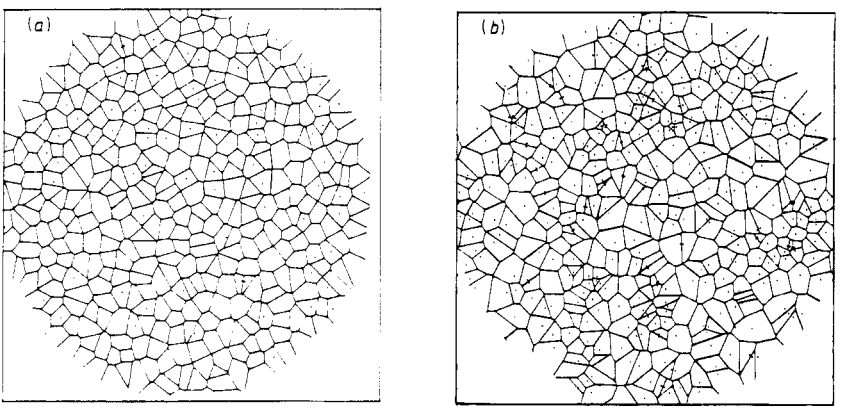

Figure 3. (a) Random matrix Voronoi froth, $N = 400$, $\sigma = 1$, (b) Random Voronoi froth, $N = 400$ points distributed according to a Poisson process in a circle of radius 20.

According to Hwang, the latter condition due to Geman (see Hwang 1986) can be weakened by tighter estimates. He further conjectured that the limiting spectral distribution of $M_N/(\sigma\sqrt{N})$ distributes uniformly over the unit disc. Sommers *et al* (1988) have also concluded that the results obtained for Gaussian ensembles for the $N \to \infty$ limit are valid for much broader classes of ensembles, without, however, specifying these classes. As noted by Sommers *et al* (1988), the projection of the eigenvalue density (constant in a disc for $N \to \infty$) on the real axis or on the imaginary axis leads to a generalised semicircle law:

$$\lambda_N(x) = (2/\pi)(N - x^2)^{1/2} \qquad |x| \leqslant N^{1/2} \tag{5}$$

(written here such that $\int_0^{\sqrt{N}} \lambda_N(x)\,dx = N/2$). This law has been used (figure 2) to check the validity of the numerical simulations (see section 3).

During the course of the present work, Grobe and Haake (1989) have published a paper in which they have shown that the type of level repulsion observed for Gaussian ensembles is universal and characterised by the fact that the distribution $P_{nn}(r)$ of nearest-neighbour spacing goes like r^3 when the distance r between two eigenvalues goes to zero.

According to Grobe and Haake (1989), the crucial property yielding universal behaviour of $P_{nm}(r)$ is:

$$W_{ij}(m_{ij}) \xrightarrow{m_{ij} \to 0} \text{constant} \qquad (\neq 0, \infty) \tag{6}$$

where W_{ij} is the distribution of the matrix element m_{ij}.

We have done many simulations with various distributions including Pareto-type distributions. They show indeed a universal behaviour but with conditions which are weaker than the condition given by (4) or by (6). By universal we mean here that the numerical characteristics of the simulated distributions of eigenvalues do not differ significantly from the characteristics of the eigenvalue distribution in the Gaussian case. In particular, the cumulative distribution $P_N(r)$ defined in subsection 3.1 (equation (9)) is the same within numerical accuracy for a large class of distributions of the matrix elements. For example, the universal distribution is obtained when one takes IID m_{ij} random variables such as:

$$\text{Prob}\{m_{ij}^x = 1/\sqrt{2}\} = \text{Prob}\{m_{ij}^x = -1/\sqrt{2}\} = 0.5 \tag{7}$$

(x = real or imaginary) with $W_{ij}(m_{ij}) = 0$ when $m_{ij} = 0$. We have observed that only the condition that the mean and the variance exist is needed to yield the universal distribution in the limit $N \to \infty$ (Le Caër 1990). It even seems that no condition at all on the moments (relation (4)) is needed in the limit $N \to \infty$. This has the consequence that there only exists one tessellation (in the statistical sense) associated with the eigenvalues of fully asymmetric complex matrices, just as there only exists one tessellation generated from a Poisson process. The random matrix Vornoi froth may therefore be used as a reference structure somewhere between complete disorder and complete order.

3. Numerical methods

3.1. Eigenvalue calculations

Random numbers distributed according to a Gaussian distribution have been obtained by the Box–Müller method (see for example Black and Kennedy 1989). Two uniform

pseudo-random numbers U, $V \in [0, 1]$ are obtained with the RANF( ) generator on a Cray-YMP/832, they are used for calculating X_1 and X_2:

$$X_1 = (-\log U)^{1/2} \cos(2\pi V) \qquad X_2 = (-\log U)^{1/2} \sin(2\pi V). \tag{8}$$

X_1 and X_2 are independently distributed according to a Gaussian distribution with mean zero and standard deviation $1/\sqrt{2}$. The matrix elements are taken as $X_1 + iX_2$, the σ of the previous section is therefore equal to 1 and the spectral radius of an $N \times N$ matrix is close to $\sqrt{N}$ (figure 3(a)).

The complex matrices are diagonalised with a vectorised subroutine F02AJF from the NAG library. The time needed to diagonalise a matrix varies as $N^{2.7}$ on one Cray processor, going from 4s for $N = 200$ to 490s for $N = 1800$. The average spectral radius obtained from 50 matrices with $N = 400$ is $S_{400} = 0.99_5 \pm 0.02$ for matrix elements distributed according to equation (7) in agreement with the conjecture of Hwang ($S_\infty = 1$) for $N \to \infty$.

Figure 2(a) presents the generalised semicircle law calculated from equation (5) with $N = 400$. It has been verified that no significant differences exist between the histograms obtained from the projections of the eigenvalues on the real and the imaginary axis. Figure 2 shows the average projection on the real axis for 50 Gaussian matrices ($(\lambda_N(x > 0) + \lambda_N(x < 0))/2$). Similar results are obtained for distribution (7) and for a uniform distribution of the real and imaginary parts between $-\sqrt{6}/2$ and $\sqrt{6}/2$ ($\sigma = 1$). Finite-size effects are observed in figure 2(a) for $x \approx 20$. The cumulative distribution function of the distance r from a point chosen at random to the nearest eigenvalue is given by $P_N(r)$ for $N \to \infty$ with

$$P_N(r) = 1 - E_N(r) = 1 - \prod_{j=1}^{N} \left(\exp(-r^2/\sigma^2) \sum_{l=0}^{j-1} \frac{(r/\sigma)^{2l}}{l!} \right) \tag{9}$$

where $E_N(r)$ has been calculated by Mehta (1967). $P_N(r)$ is estimated from simulations by using methods described by Ripley (1981, chapter 8). The theoretical $P_N(r)$ is calculated from equation (9). The product in (9) converges rapidly (see also Grobe *et al* 1988). Figure 2(b) demonstrates the excellent agreement (better than 0.5%) between simulation and theory (similar results are obtained for N as small as ~50).

3.2. Voronoi tessellations

The computation of Voronoi tessellations from RVF or from eigenvalues of complex random matrices (RMVF) has been done with an algorithm which first constructs the Delaunay tessellation. This algorithm is an adaptation for $D = 2$ (Ho, unpublished) of the algorithm of Tanemura *et al* (1983) for $D = 3$. Periodic boundary conditions are used with respect to a square of side $2S_N\sqrt{N}$ where S_N is the spectral radius defined in section 2. This produces very elongated cells mainly at the corners of the square. As explained below, these cells are not used in the statistical study. They have been deleted from figure 3.

Very recently, Telley (1989) has used the Voronoi tessellation in the Laguerre geometry (Imai *et al* 1985). In the latter geometry, points are replaced by circles in the plane and the distance from a point to a circle is defined by the length of the tangent line.

The repulsion effect, which gives rise to a more regular tessellation, is clearly seen by comparison between figure 3(a) and 3(b). We present in table 1 the distributions

p_n of the number of sides of the Voronoi polygons for the cucumber froth of figure 1 and for the RMVF and RVF.

The variance $\mu_2 = \langle n^2 \rangle - \langle n \rangle^2$ is 0.64, 1.23 and 1.78 for the cucumber, RMVF and RVF respectively. The proportions of cells with four, six or eight sides clearly differ for the first two froths.

In order to study the statistical properties of the RMVF and RVF, it would be best to use the method of Hinde and Miles (1980) who have simulated 2×10^6 cells for a RVF. They have calculated the properties of the central cell generated in a fixed area from n points, where n is distributed according to a Poisson distribution with a mean $\langle n \rangle = 100$. As we do not know the distribution of the number of eigenvalues in a given area for a given ρ beforehand, we have chosen to fix a matrix size $N = 500$ and to study only as a mean 60% of the cells contained in a circle of fixed radius $R = 17.32$, while $S_{500} \approx 22.36$.

This method, which at first sight may not be considered a good method because it would be necessary to also let N fluctuate, has been used for the Poisson process in the same conditions. The results of section 4 will in fact show that it works quite accurately for the random Voronoi froth. As the fluctuation of the number of eigenvalues in a fixed area and for a given density are expected to be smaller for the RMVF than for RVF, the previous agreement strongly supports the validity of our numerical results which are also further confirmed by some simple checks (section 4).

Three simulations have been performed in the first case and five in the second case, with respective number of cells N_c:

(i) RVF: $N_c = 600\,696$, $N_c = 1001\,500$, $N_c = 1020\,800$.

(ii) RMVF: $N_c = 90\,303$, $N_c = 80\,409$, $N_c = 25\,600$ for $N = 500$, $N_c = 48\,026$ and $N = 400$, $N_c = 59\,977$ for $N = 600$ (but with, as a mean, 50% of the eigenvalues).

Some satistical properties of the Delaunay tessellations have also been calculated but only for one simulation.

4. Numerical results

4.1. Random Voronoi froth

In the following, all quantities are the averages performed over the simulation results and the quoted error represents one standard deviation estimated from them. All parameters have been normalised by multiplying by a factor whose value is known theoretically (Stoyan *et al* 1987, Miles 1970) as a function of the density ρ. This factor is ρ for the cell area (a), $\sqrt{\rho}/4$ for the cell perimeter (s) and $6\sqrt{\rho}/4$ for the cell side length (l). For Delaunay tessellation, the normalisation factor is 2ρ, $3\pi\sqrt{\rho}/32$ and $9\pi\sqrt{\rho}/32$ for the area (A), the perimeter (S) and the side length (L). Table 2 gives $\langle X \rangle$, $\langle X^2 \rangle$ for the previous parameters and for the cell side number n. The average number of sides m_n of cells in contact with n-sided cells and the average of normalised area $\langle a(n) \rangle$ (tables 5 and 7) are used to discuss the Aboav-Weaire law (section 5) and the Lewis-Rivier law (section 6). The distribution p_n of the number of sides (table 1) is in very good agreement with the distributions calculated numerically by Hinde and Miles (1980) and Drouffe and Itzykson (1984). The latter authors have obtained theoretical expressions involving integrals for p_n and $\langle a(n) \rangle$. Drouffe and Itzykson have calculated these integrals by the Monte Carlo method and obtained the previous quantities without simulating cells. The very good agreement between their results and

Table 2. Average, second moment, standard deviation for the area, the perimeter, the side length, the side number (A, S, L are for the Delaunay tessellation). Values $\langle X^2\rangle^*$ from other numerical sumulations (NS) or from theoretical calculations (T).

X	$\langle X\rangle$	$\langle X^2\rangle$	$\langle X^2\rangle^*$	Reference for $\langle X^2\rangle^*$	σ_x
a	0.9998 (4)	1.277 (1)	1.280	T, Gilbert 1962	0.5267 (5)
s	1.0002 (4)	1.0586 (4)	1.0601	NS, Hinde and Miles, 1986	0.2420 (4)
l	1.0003 (4)	1.417 (1)	1.418	T, quoted by Boots 1987	0.646 (1)
n	5.99998 T, 6	37.781 (3)	37.783	NS, Hinde and Miles 1980	1.334 (1)
A	1.0004	1.769	1.77312	T, Miles 1970	0.877
S	1.0007	1.150	1.15048	T, Miles 1970	0.387
L	1.0004	1.2425	1.24252	T, Miles 1970	0.492

ours confirm the validity of our simulation method for $n < 12$. Figure 4 shows the distribution of the normalised side length l, $Q(x_i) = \int_{x_i}^{x_i+0.02} q(l)\,\mathrm{d}l$, with a bin size of 0.02. For $x_i = 0$, the average $Q(0)$ obtained for three simulations is $0.010\,25 \pm 0.000\,23$ which gives $q(0) = 0.512 \pm 0.012$, as $Q(x_i)$ is almost constant for small lengths. Boots (1987) has obtained $q(0) = 0.493$ from a simulation with 30 000 polygons. The value $q(0) = 0.46$ which is given by Crain (1978) is too small, as already discussed by Boots.

The distribution of the absolute value l of a Gaussian variable $N(m_l, \sigma_l^2)$ is given by ($l \geq 0$)

$$q_l(l) = \frac{1}{\sigma_l\sqrt{(2\pi)}}\left[\exp\left(-\frac{(l-m_l)^2}{2\sigma_l^2}\right) + \exp\left(-\frac{(l+m_l)^2}{2\sigma_l^2}\right)\right]. \tag{10}$$

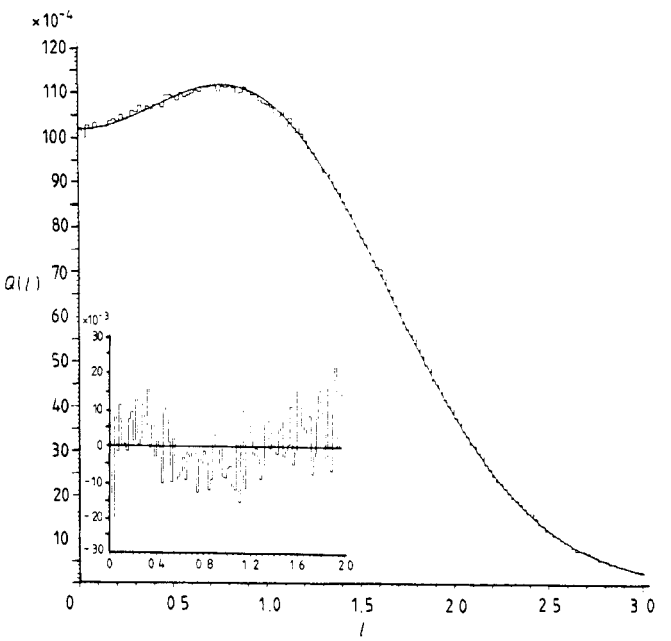

Figure 4. Distribution of the normalised cell length side l for a random Voronoi froth (histogram: simulation with 10^6 cells, full curve: empirical shape $Q_l(l)$ of subsection 4.1). Inset: relative deviation between the two histograms for l less than 2.

The first two moments are

$$\langle l \rangle = \left(\frac{2}{\pi}\right)^{1/2} \sigma_l \exp\left(-\frac{m_l^2}{2\sigma_l^2}\right) + m_l \operatorname{erf}\left(\frac{m_l}{\sigma_l\sqrt{2}}\right) \tag{11}$$

$$\langle l^2 \rangle = \sigma_l^2 + m_l^2 \tag{12}$$

where erf is the error function. For some combination of m_l and σ_l, this distribution has a shape which is similar to the shape of $q(l)$. From $\langle l \rangle = 1$ and $\langle l^2 \rangle = 1.4172$, we deduce $m_l = 0.9144$ and $\sigma_l = 0.7623$ $(m_l/\sigma_l = 1.20)$ and we calculate $Q_t(x_i) = \int_{x_i}^{x_i+0.02} q_t(l)\,\mathrm{d}l$. The full curve of figure 4 passes through the midpoints of the calculated bins. The deviation between Q and Q_t is at most of the order of 2% and has an average absolute value of 0.7% for l less than 2.5 and 1% for l less than 3. The value of $q_t(0)$ is 0.5098.

Table 3. Average, second moment, standard deviation for the area, the perimeter, the side length, the side number (A, S, L are for the Delaunay tessellation) in the random matrix case.

X	$\langle X \rangle$	$\langle X^2 \rangle$	σ_x
a	$1 \pm 3 \times 10^{-4}$	1.0570 (2)	0.239 (1)
s	1.0022 (5)	1.0132 (5)	0.1038 (4)
l	1.0022 (5)	1.338 (2)	0.580 (2)
n	6.0005 (9)	37.23 (1)	1.110 (7)
A	1.0003	1.248	0.498 (1)
S	1.0108	1.059	0.220 (2)
L	1.0108	1.118	0.328 (1)

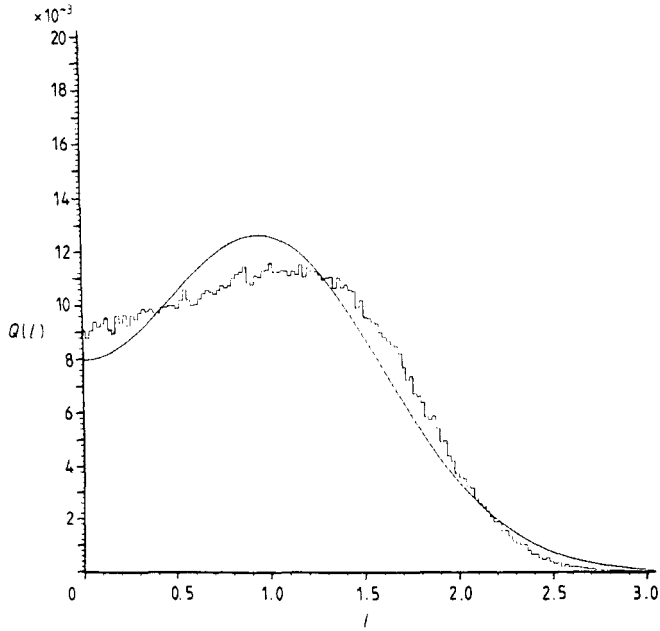

Figure 5. Distribution of normalised cell length l (normalisation factor $1.5\sqrt{\rho}$) for a random matrix Voronoi froth, histogram: simulation with 90 303 cells, full curve: equation (10) (which is invalid for the RMVF).

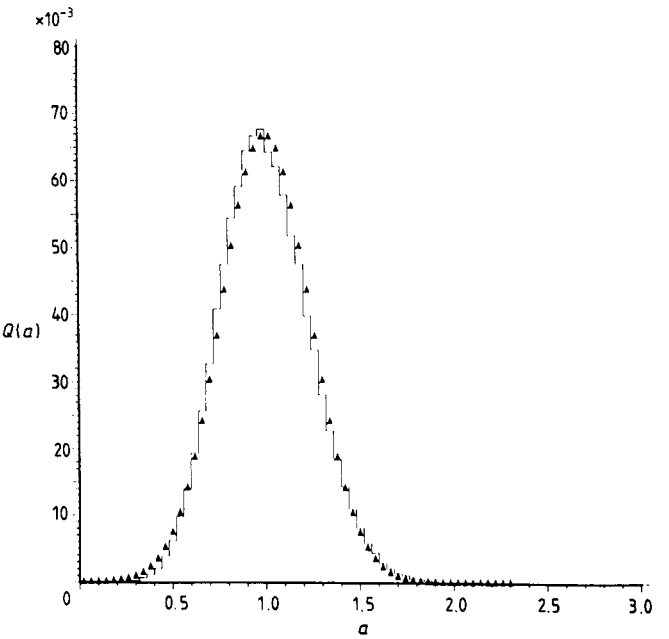

Figure 6. Distribution of the normalised area for the random matrix Voronoi froth (full triangles: histogram calculated for a normal distribution with $m = 1$ and $\sigma = 0.2385$).

4.2. Random matrix Voronoi froth

No theory exists for the parameters described in this section, except that we trivially expect that $\langle n \rangle = 6$ and that the normalisation factor for the area is the density ρ. We have kept the normalisation factors of the previous section for the perimeter and the side length of the cells in the Voronoi and Delaunay tessellations. Table 3 shows that the averages are almost 1 and table 1 gives the proportions p_n of n-sided cells.

Figure 5 presents the side length distribution. The empirical shape of subsection 4.1 does not fit the simulated distribution ($m_l = 0.9658$, $\sigma_l = 0.6392$). The distribution is narrower than the corresponding RVF distribution and $q(0)$ is smaller ($q(0) = 0.45 \pm 0.01$). Figure 6 finally shows the distribution of the normalised area as well as a Gaussian approximation to it. It is not a gamma function of the form $a^{\gamma-1}\exp(-\gamma a)$ as it is for a RVF ($\gamma \approx 3.60$, Weaire *et al* 1986, DiCenzo and Wertheim 1989).

5. Aboav–Weaire law

In two dimensions there are only two elementary structural transformations: neighbour switching and face disappearance (Weaire and Rivier 1984). As emphasised by Rivier (1985), the latter transformation cannot occur in a 2D Voronoi froth as the number of seeds is conserved. The Aboav-Weaire law expresses that the average number, m_n ($= \overline{m(n)}$), of sides of cells adjacent to n-sided cells is approximately linearly related to $1/n$ by

$$m_n = A + B/n. \tag{13}$$

A linear law is in fact obtained with $A = 5$ and $B = 6$ (Weaire 1974) from the average turning angle of a grain. Weaire also established a sum rule

$$\langle n m_n \rangle = \mu_2 + 36 = \langle n^2 \rangle \tag{14}$$

where μ_2 is the variance of n, $\mu_2 = \langle n^2 \rangle - \langle n \rangle^2$. As the experimental B values were different from 6, Weaire (1974) proposed to include μ_2 in B and later Aboav (1980) proposed to express (13) as

$$m_n = 6 - a + (6a + \mu_2)/n. \tag{15}$$

Blanc and Mocellin (1979) have studied the evolution of a froth under the two elementary structural transformations, assuming no correlation beyond nearest neighbours (see also Rivier 1985). They have thus obtained the linear law (15) with $a = 1$. Very recently, Fortes and Andrade (1989) have constructed a network from randomly distributed straight lines. They obtain a very large second moment value $\mu_2 = 9.11$. The m_n variation is still well represented by the Aboav-Weaire law (15) for $a = 0.35$. They conclude to the general applicability of the law to random networks.

Table 4 gives the values of m_n obtained in the present work for the RVF as well as the values published by Boots and Murdoch (1983) for 50 000 cells.

Table 4. Values of m_n for the random Voronoi froth.

n	Boots and Murdoch (1983)	Present work	Equation (15) $a = 0.586$	Equation (22)
3	7.013	7.009 (3)	7.180	7.036
4	6.731	6.718 (3)	6.738	6.707
5	6.493	6.492 (1)	6.473	6.485
6	6.312	6.315 (2)	6.297	6.316
7	6.169	6.171 (1)	6.171	6.176
8	6.048	6.050 (1)	6.076	6.056
9	5.932	5.948 (2)	6.003	5.949
10	5.841	5.859 (1)	5.944	5.850
11	5.779	5.78 (1)	5.896	5.758

No results have been published on $\overline{m^2(n)}$. We have calculated $\sigma_m^2(n) = \overline{m^2(n)} - m_n^2$ ($m_n = \overline{m(n)}$) and found that, to a very good approximation,

$$\sigma_m(n) = \alpha(m_n - \beta) \tag{16}$$

in the investigated range of n, with $\alpha = 0.241$ and $\beta = 4.723$ for the RVF. Using sampling theory, we obtain an estimate, in the statistical sense, of the standard deviation on the m_n values of table 4:

$$\sigma^*(n) = \sigma_m(n)/\sqrt{sN_c p_n} \tag{17}$$

where s is the number of simulations with N_c cells which have been used to calculate m_n. In the present work, $N_c = 10^6$ for two simulations and $N_c = 6 \times 10^5$ for the last one (subsection 3.2).

Using equations (16) and (17), we can calculate $\sigma^*(n)$ in particular for $n = 3$, $n = 9$ and $n = 10$, which represent only about 4% of the cells. We obtain $\sigma^*(3) = 0.003$, $\sigma^*(9) = 0.001$ $\sigma^*(10) = 0.002$ in agreement with the values of table 4, which have been estimated directly from the experimental results. We conclude that the m_n values can be used to check the Aboav-Weaire law even for p_n values as low as $\sim 0.5\%$.

There is no value of a in (15) which is able to account within numerical accuracy for the results of table 4. If we evaluate

$$a_n = (nm_n - 6n - \mu_2)/(6 - n) \tag{18}$$

we obtain values ranging from 0.415 (3) for $n = 3$ to 0.800 (5) for $n = 10$ with systematic behaviour and no fluctuations around a constant as would be expected if equation (15) were valid.

If we fit the 'experimental' m_n with (15), using a least-squares method for $n = 4$–8, we obtain $a = 0.586$. Differences larger than ten times the standard deviation exist between the calculated and 'experimental' m_n for $n = 3, 5, 8, 9$ (table 4). Equation (15) shows that m_6 does not depend on a and is:

$$m_6 = 6 + \mu_2/6 \tag{19}$$

i.e. $m_6 = 6.297$ (1) instead of 6.315 (2). In other words, a μ_2 value of 1.89 (1) would be needed instead of 1.781 (3) in order to account for the 'experimental' m_6. A weighted least-squares fit, using all n values, gives $a = 0.618$. We conclude that there exist deviations from the Aboav-Weaire law in the RVF. This agrees with a remark of Rivier (1985), who suggests that the RVF may not be topologically stable with shape correlation extending beyond nearest neighbours. According to Kawasaki (1990), his recent simulations for studying the kinetics of grain growth confirm the link, first established theoretically by Blanc and Mocellin (1979), between the Aboav-Weaire law and correlations restricted to nearest-neighbour cells.

In order to overcome these discrepancies, Aboav (1987) has proposed for the RVF an empirical equation free from arbitrary constants:

$$m_n = \langle n \rangle + 2/n + \tfrac{1}{2}(\langle n^{1/2} \rangle - n^{1/2}) \tag{20}$$

($\langle n^{1/2} \rangle = 2.4343$ (7) from the present work). Equation (20) better fits the observed values than (15), but it presents two main drawbacks:

(i) it departs too much from the basic linear law;

(ii) it is not valid for all tessellations. The sum rule (14) applied to equation (20) requires that (Aboav 1987):

$$\mu_2 = 2 + \tfrac{1}{2}(6\langle n^{1/2} \rangle - \langle n^{3/2} \rangle).$$

This is approximately true for the RVF, but for the RMVF $\mu_2 = 1.23$ (2) while the right-hand side is 1.88 (1). In fact, (20) does not fit at all the m_n values of table 5. It may be better to try to add small correction terms to (15). A plot of nm_n as a function of n for the RVF or for the RMVF (figure 7) clearly shows a downwards curvature.

In order to get a numerical evaluation of the deviations from the linear law, we expand nm_n as a function of n up to n^2:

$$m_n = A + B/n + Cn. \tag{21}$$

Table 5. Values of m_n for the random matrix Voronoi froth.

	$n = 3$	$n = 4$	$n = 5$	$n = 6$	$n = 7$	$n = 8$	$n = 9$	$n = 10$	$n = 11$
Simulation	7.21 (4)	6.770 (9)	6.462 (8)	6.217 (7)	6.020 (9)	5.860 (7)	5.724 (7)	5.60 (1)	5.47 (4)
Equation (15), $a = 1.136$	7.543	6.873	6.471	6.203	6.012	5.869	5.757	5.668	5.595
Equation (22), $a = 0.62$ $b = 7.23 \times 10^{-2}$	7.258	6.774	6.455	6.218	6.028	5.868	5.727	5.600	5.483

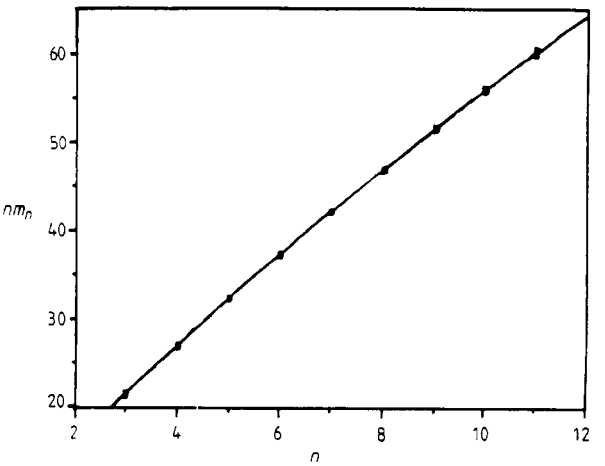

Figure 7. Values of nm_n for the random matrix Voronoi froth (solid rectangles) and fit with equation (22) (full curve).

In the previous expansion it is easy to take the sum rule (14) into account using only $\langle n \rangle$ and $\langle n^2 \rangle$, as done for (15). We obtain:

$$m_n = 6 - a + b(6 + \mu_2/6) + (6a + \mu_2)/n - bn. \tag{22}$$

Other sum rules, which are not so easily taken into account, have been established by Lambert and Weaire (1983). A fit of m_n with (22) gives $a = 0.2332$ and $b = 6.343 \times 10^{-2}$ (table 4). Equation (22) cannot be valid for all values of n, as m_n would become negative for $n \simeq 195$ (but p_{50} is only of the order of 10^{-75} (Drouffe and Itzykson 1984)).

Equation (16) also holds for $\sigma_m(n)$ in the RMVF with $\alpha = 0.162$ and $\beta = 4.542$. Using all the simulations with various N_c values, we calculate $\sigma^*(3) = 0.02$, $\sigma^*(9) = 0.004$ and $\sigma^*(10) = 0.008$ from (17), in reasonable agreement with the deviations given in table 5. We notice that σ_m decreases with n and that the condition $\sigma_m \geqslant 0$ and the Aboav-Weaire law give $a \leqslant 6 - \beta$, which is 1.46 for the RMVF. This upper limit is in fact quite close to the values of a which are obtained in many natural random cellular structures $a \sim 1.2$ (Aboav 1980, 1984) and in the present work for the RMVF.

A weighted fit with the linear law gives $a = 1.14$ for the RMVF. The a_n calculated from (18) vary between 0.79 (4) for $n = 3$ and 1.41 (6) for $n = 11$ with a mean which is in fact close to the previous value of a. A fit with (22) gives $a = 0.62$, $b = 0.0723$.

Although the linear law is a better approximation for the RMVF than for the RVF, we still observe significant deviations mainly for $n = 3, 4$ (table 5). Similar observations are reported by Kawasaki (1990) in his simulations of grain growth. A different approach has been used by Boots and Murdoch (1983) which consists in replacing the Cn term in (21) by a C/n^2 term. This form is in fact valid whatever n and the application of the sum rule (14) yields

$$m_n = 6 - a + b\tfrac{1}{6}\langle 1/n \rangle + (6a + \mu_2)/n - b/n^2. \tag{23}$$

In the range of n which is accessible in the present studies, (22) and (23) give fits of comparable accuracy. Considering the b/a values obtained for the RVF and RMVF (0.272 and 0.116 (equation (22)) and 8.42 and 7.91 (equation (23)), respectively), it is

tempting to relate this parameter to the ageing of the structure which changes the shape correlations of cells. The equilibrated froth may correspond to $b/a = 0$ if one further considers the distributions of the normalised length of cell sides l which may show a small or zero probability for $l = 0$. Aboav (1980) has studied soap froths at different stages of their growth with about 15 h between two successive stages. His results show a change of the curvature of m_n as a function of n from downwards to upwards as a function of time, particularly for small values of n. Unfortunately, the numbers of cells which are used to determine m_n are too small to give a significant test of the deviation from the linear law. In conclusion, the present section suggests investigating more precisely the deviations from the linear Aboav-Weaire law in natural structures. These deviations mainly occur outside the range $n = 5$-8. This may help to define new constraints in statistical crystallography.

6. Lewis–Rivier law

This law relates the average normalised area $\langle a_n \rangle$ of n-sided cells linearly to n

$$\langle a_n \rangle = (n - n_0)/(6 - n_0) \tag{24}$$

which gives, as expected, $\langle\langle a_n \rangle\rangle_n = 1$. It was first proposed by Lewis (1928). Rivier has later shown (Rivier 1983, 1985) that the 'ideal' structure, in the sense of statistical crystallography, corresponds to the minimal number of constraints and has Lewis' law as its equation of state. This law allows the maximising of the entropy. For equilibrium structures, δ ($n_0 = 6 - 1/\delta$) measures their ageing (Rivier 1985).

Figure 8 of the present paper and figure 4 of Drouffe and Itzykson (1984) show that $\langle a_n \rangle$ varies linearly with n for $n < 11$ in a RVF. A clear change of slope is obtained

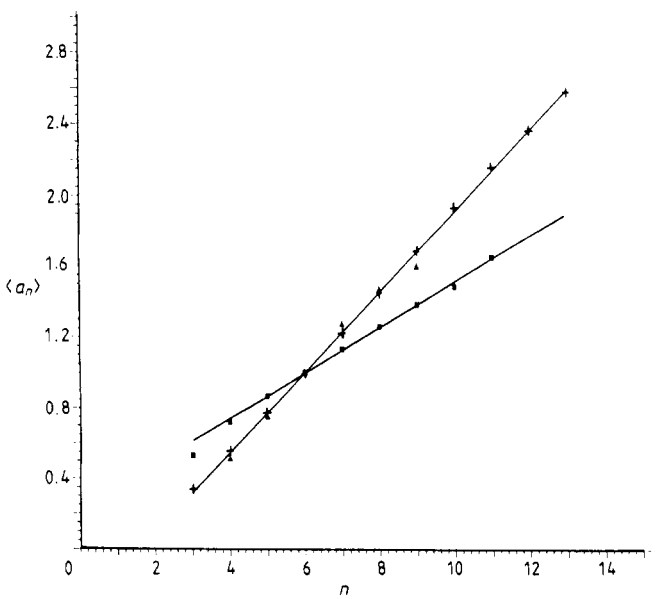

Figure 8. Normalised area of n-sided cells $\langle a_n \rangle$ as a function of n for the cucumber froth (solid triangles, Lewis 1928), the RVF (crosses) and the RMVF (solid squares).

Table 6. Average normalised area $\langle a_n \rangle$ as a function of n for the RVF and the RMVF.

	$n=3$	$n=4$	$n=5$	$n=6$	$n=7$	$n=8$	$n=9$	$n=10$	$n=11$	$n=12$	$n=13$
RVF†	0.342 (1)	0.560 (1)	0.777 (1)	0.996 (1)	1.228 (1)	1.463 (2)	1.693 (3)	1.930 (6)	2.155 (8)	2.400 (9)	2.691 (11)
RVF‡	0.342 (2)	0.558 (2)	0.774 (1)	0.996 (2)	1.222 (1)	1.451 (2)	1.688 (2)	1.938 (2)	2.16 (3)	2.37 (5)	2.6 (2)
RMVF‡	0.53 (1)	0.721 (3)	0.869 (1)	1.003 (1)	1.133 (1)	1.259 (3)	1.382 (9)	1.50 (2)	1.65 (4)	—	—

† Drouffe and Itzykson (1984).
‡ Present work.

by the latter authors for $n > 12$. From table 6 we obtain $n_0 = 1.6$ for RVF and accidentally a similar value for the cucumber froth $n_0 = 1.9$ (for n varying from 4-8) as seen in figure 8. For the RVF, n_0 was believed to be $n_0 \sim 0$, as established from the data of table 3 of Crain (1978). Boots (1987) has first suggested that the columns for the average second moment of the perimeter and for the average area have been transposed in the Crain's paper. This is in complete agreement with the results of the present work (table 6).

For the RMVF, the largest linear part of $\langle a_n \rangle$ against n gives $n_0 = -1.78$. We conclude than one cannot interpret the n_0 values for both Voronoi froths in the frame of the Rivier statistical theory because they are not equilibrated.

7. Discussion

As for the RVF, the Voronoi tessellation generated from the eigenvalues of complex matrices which have no particular kind of symmetry, has not fully equilibrated under the influence of constraints. In the language of Rivier (1985), it is also a young structure but not as young as the RVF. The RMVF may thus be relaxed, even more rapidly than the RVF, to a structure similar to natural structures. Three elements support these arguments:

(i) the distributions of the number of sides (table 1);

(ii) the b/a values of the Aboav-Weaire law are large but $(b/a)_{\mathrm{RMVF}} < (b/a)_{\mathrm{RVF}}$;

(iii) the probability for short edges is large but $q(0)_{\mathrm{RMVF}} < q(0)_{\mathrm{RVF}}$.

The formation of a dip in this distribution at $l = 0$ may be expected and is observed for natural and equilibrated structures.

Although we do not know if the following remark has any significance, we observe that the behaviour of the side length l reminds us, at least formally, the behaviours of local field distributions $P(h)$ in spin glasses (Thomsen *et al* 1986, Binder and Young 1986) with a more and more pronounced dip in $P(h)$ for $h = 0$ and $T \to 0$. A further similarity is that the empirical $q(l)$ distribution of subsection 4.1. (equation (10)) is the theoretical shape of $P(h)$ for a temperature higher than the spin-glass temperature in an infinite-ranged Ising spin glass (Thomsen *et al* 1986). It also nicely fits simulation results of Binder (figure 73, Binder and Young 1986) for the nearest-neighbour symmetric Gaussian model (Le Caër, unpublished results).

The present work confirms the importance of the Aboav-Weaire law but brings some corrections which may be used to follow the evolution of cellular structures.

8. Conclusion

The universal distribution of eigenvalues of fully asymmetric complex random matrices allows the defining of a unique tessellation. The repulsion effect between eigenvalues gives rise to a structure which is more regular than the random Voronoi froth and which looks at first glance like some natural mosaics. However, the deviation with respect to the Aboav-Weaire law and the distribution of cell-side length allow one to conclude that the random matrix Voronoi froth is still a young, not completely equilibrated, structure in the sense of the statistical crystallography theory of Rivier. This froth may also serve as a reference tessellation.

Geometrical and topological distributions have been characterised both for the random Vornoi froth and the random matrix Voronoi froth. An empirical and accurate distribution function has been proposed for the side length of the polygons in a random Voronoi froth. Deviations from the Aboav-Weaire law which occur outside the range $n = 5$-8 have been discussed.

Acknowledgments

We thank HLRZ for its hospitality and support for the three movements of this cell concerto. GLC also thanks CNRS for having financed a one-year stay in Jülich. We thank A Mocellin (Ecole des Mines, Nancy) and R A Brand (IFF, KFA Jülich) for useful discussions, D Stauffer and H Herrmann for a critical reading of the manuscript.

References

Aboav D A 1970 *Metallography* **3** 383-90
—— 1980 *Metallography* **13** 43-58
—— 1984 *Metallography* **17** 383-96
—— 1987 *Acta Stereol.* **6/III** 371-3
Binder K and Young A P 1986 *Rev. Mod. Phys.* 801-976
Black S C and Kennedy A D 1989 *Computers in Physics* May/June 1989 59-67
Blanc M and Mocellin A 1979 *Acta Metall.* **27** 1231-7
Boots B N 1987 *Metallography* **20** 231-6
Boots B N and Murdoch D J 1983 *Computers and Geosciences* **9** 351-65
Christ N H, Friedberg R and Lee T D 1982 *Nucl. Phys.* B **202** 89-125
Crain I K 1978 *Computers and Geosciences* **4** 131-41
De Almeida R M C and Iglesias J R 1988 *J. Phys. A: Math. Gen.* 3365-77
—— 1989 *Phys. Lett.* **138A** 253-7
DiCenzo S B and Wertheim G K 1989 *Phys. Rev.* B **39** 6792-6
Drouffe J M and Itzykson C 1984 *Nucl. Phys.* B **235** 45-53
Fortes M A and Andrade P N 1989 *J. Physique* **50** 717-24
Getis A and Boots B N 1979 *Models of Spatial Processes* (Cambridge: Cambridge University Press)
Gilbert E N 1962 *Ann. Math. Stat.* **33** 958-72
Ginibre J 1965 *J. Math. Phys.* **6** 440-9
Grobe R and Haake F 1989 *Phys. Rev. Lett.* **62** 2893-6
Grobe R, Haake F and Sommers H J 1988 *Phys. Rev. Lett.* **61** 1899-902
Hinde A L and Miles R E 1980 *J. Stat. Comput. Simul.* **10** 205-23
Honda H 1978 *J. Theor. Biol.* **72** 523-43
Hwang C R 1986 *Random Matrices and Their Applications* ed J E Cohen, H Kesten and C M Newman (*Contemporary Mathematics* **50**) (Providence, RI: American Mathematical Society) pp 145-52
Imai H, Iri M and Murota K 1985 *Siam J. Comput.* **14** 93-105

Kawasaki K 1990 *Physica* A **163** 59-70
Lambert C J and Weaire D 1983 *Phil. Mag.* B **47** 445-50
Le Caër 1990 in preparation
Lewis F T 1928 *The Anatomical Record* **38** 341-76
Mehta M L 1967 *Random Matrices and the Statistical Theory of Energy Levels* (New York: Academic)
Meijering J L 1953 *Philips Res. Rep.* **8** 270-90
Miles R E 1970 *Math. Biosci.* **6** 85-127
Quine M P and Watson D F 1984 *J. Appl. Prob.* **21** 548-57
Ripley B D 1981 *Spatial Statistics* (New York: Wiley)
Rivier N 1983 *Phil. Mag.* B **47** L45-9
—— 1985 *Phil. Mag.* B **52** 795-819
Rivier N and Lissowski A 1982 *J. Phys. A: Math. Gen.* **15** L143-8
Seligman T H and Nishioka H (eds) 1986 *Quantum Chaos and Statistical Nuclear Physics* (*Lecture Notes in Physics* **263**) (Berlin: Springer)
Sommers H J, Crisanti A, Sompolinsky H and Stein Y 1988 *Phys. Rev. Lett.* **60** 1895-908
Stoyan D, Kendall W S and Mecke J 1987 *Stochastic Geometry and its Applications* (New York: Wiley)
Tanemura M, Ogawa T and Ogita N 1983 *J. Comput. Phys.* **51** 191-207
Telley H 1989 *Thesis* (no 780) Ecole Polytechnique Fédérale de Lausanne Switzerland
Thomsen M, Thorpe M F, Choy T C, Sherrington D and Sommers H J 1986 *Phys. Rev.* B **33** 1931-47
Weaire D 1974 *Metallography* **7** 157-60
Weaire D, Kermode J P and Wejchert J 1986 *Phil. Mag.* B **53** L101-5
Weaire D and Rivier N 1984 *Contemp. Phys.* **25** 59-99
Wray P J, Richmond O and Morrison H L 1983 *Metallography* **16** 39-58